

# The spectral dependence of facular contrast and solar irradiance variations

Y.C. Unruh<sup>1</sup>, S.K. Solanki<sup>2</sup>, and M. Fligge<sup>2</sup>

<sup>1</sup> Institut für Astronomie, Universität Wien, Türkenschanzstrasse 17, A-1180 Wien, Austria

<sup>2</sup> Institute of Astronomy, ETH-Zentrum, CH-8092 Zürich, Switzerland

Received 12 October 1998 / Accepted 1 March 1999

**Abstract.** We present model calculations of facular and sunspot contrasts as a function of wavelength and limb angle on the Sun. These are the first such calculations; they assume LTE and are based on opacity distribution functions (ODFs). The calculated facular contrasts as a function of limb angle fit into the general picture of contrast measurements, and the behaviour of the contrast with wavelength at a given limb angle is in excellent agreement with the measurements.

The calculated intensity spectra are used to construct the solar flux spectrum for different levels of solar activity. It is assumed that the irradiance or flux variations are due to changes in the sunspot and facular filling factors. The model atmosphere used to calculate the facular intensities has been tuned so that the calculated irradiance variations match the observed total and spectral irradiance variations during the last solar cycles.

The model calculations have also been used to estimate the relative importance of continuum and spectral-line variations in producing irradiance variations. The results suggest that the continuum variations only contribute negligibly to the total irradiance variations on solar-cycle time scales.

**Key words:** Sun: activity – Sun: faculae, plages – Sun: photosphere – Sun: sunspots – Sun: UV radiation

## 1. Introduction

In a previous paper (Solanki & Unruh 1998, henceforth Paper I), we have shown that the spectral irradiance variations cannot be modelled by a simple temperature increase alone. They can be relatively well fitted, however, with a three-component model consisting of quiet-sun, spot and facular contributions. Our earlier approach was relatively crude in the way the active flux was calculated: it relied on the simplifying assumptions that the flux was given by Planck's function at each wavelength point and that the formation height of the quiet-sun and the facular contributions was the same.

The simple model of Paper I was compared with a far wider variety of data by Fligge et al. (1998, henceforth Paper II). On the whole, the model fared reasonably well, sug-

gesting that the basic approach is sound. There were, however, differences to the observations that demanded improvements. In this paper, we drop some of the original simplifications and model the different contributions much more accurately. While the assumption of LTE is kept, we now calculate the intensities and fluxes using Kurucz's ATLAS9 (Kurucz 1992a; Castelli & Kurucz 1994) spectral synthesis code. In addition, we also present the first calculations of the spectral facular contrast as a function of limb distance. These results are compared with the relevant observations.

Knowledge of the spectral facular contrast as a function of limb angle is an important ingredient when modelling the irradiance from a known surface distribution of faculae and spots. There is considerable debate about the plage contributions to the Sun's irradiance variations, and in particular about the question of whether an additional contribution, arising e.g. from latitude-dependent temperature changes (Kuhn et al. 1985, 1988; Kuhn & Libbrecht 1991) or from changes in the magnetic network (Foukal et al. 1991), is needed. The current paper is the next step in improving the modelling and understanding of spectral irradiance variations. We stress, however, that we do not use the centre-to-limb variations of the spectral facular contrast to reconstruct the irradiance in this paper. This will be the subject of a further publication.

In the following section we introduce our model. We then calculate the intensities of the different components. Sect. 3 compares the model limb-dependent intensities of the quiet Sun to the observations of Neckel & Labs (1994) and Sect. 4 looks at the colour dependence and the limb behaviour of the facular contrast. In Sect. 5 we integrate the intensities to obtain fluxes and proceed to compare our results with disk-integrated solar data in an analysis similar to the one performed in Papers I and II.

## 2. The model

Our model has three components, namely a quiet-sun, a facular and a spot contribution (see Paper II for details). In order to calculate fluxes, intensities and limb-dependent contrasts of each of these components, we employ Kurucz's ATLAS9 program with opacity distribution functions (ODFs). The program (as rewritten by J. B. Lester) and the ODFs were obtained through CCP7 (Collaborative Computing Project No. 7). Kurucz's so-

lar model atmosphere was used to obtain the quiet-sun fluxes and intensities (Kurucz 1992a, 1992b, 1992c). Our approach to modelling solar irradiance variations, although in many ways similar to that taken by Fontenla et al. (1999), is also complementary to theirs. They model selected parts of the spectrum using NLTE and, where necessary partial redistribution, thus achieving much greater realism than our LTE approach. However, the simplification of LTE and the use of ODFs allows us to calculate the whole spectrum from 160 nm to 160 000 nm with a spectral resolution of better than 200 in the visible. Whereas in theory, we are able to calculate the solar spectrum down to about 10 nm, the discrepancies between the calculated and observed solar spectrum become prohibitively large below 160 nm, so that we do not consider this extreme UV region in our comparisons. The spot fluxes (from umbra and penumbra together) were calculated from a model atmosphere of 5150 K which in turn was interpolated from the Kurucz grid of model atmospheres. Using separate models for umbra and penumbra produced no significant changes in the emerging spectrum.

Rather than making up the facular model atmosphere from scratch, we used model P of Fontenla et al. (1993) (FAL P) as a starting point. Following very small modifications, this model had proved remarkably successful in our previous attempt to model the spectral irradiance variations (see Papers I and II).

The model as used in Papers I and II had to be further altered in order to be used with ATLAS9. The original hot chromosphere produced strong excess emission in the UV as well as emission reversals in all the Balmer lines and in numerous UV lines, due mainly to the simplification of LTE that we employ. We therefore truncated the atmosphere at about the temperature minimum and extrapolated down to lower temperatures (using ATLAS9). The resulting model was then further adjusted to improve the fits to the spectral irradiance variations (see Sect. 5.1) and to the VIRGO data (see Sect. 5.2). The modifications consisted mainly in a small temperature decrease in the deeper atmospheric layers, along with a flatter temperature gradient between optical depths 0.002 and 0.4 (i.e. column masses of 0.1 to 3). The original model P as well as our current facular model are shown in Fig. 1.

### 3. The quiet photosphere: centre-to-limb variations

Before we determined the facular contrast as a function of limb angle, we first checked the centre-to-limb variation (CLV) of the intensity at different wavelengths produced by the quiet-sun model against the measurements made by Neckel & Labs (1994). This allows us to test in how far the intensity calculations approach the solar behaviour at all limb angles, and can give us a rough indication of the importance of effects that we have neglected, such as non-LTE, granulation and other inhomogeneities.

The dashed line in Fig. 2a shows the disk-integrated flux divided by the intensity at disk centre as measured by Neckel & Labs (1994) (see their Fig. 3a) and the solid line shows the same quantity as obtained with ATLAS9 and the radiative-equilibrium solar model atmosphere of Kurucz (1992a).

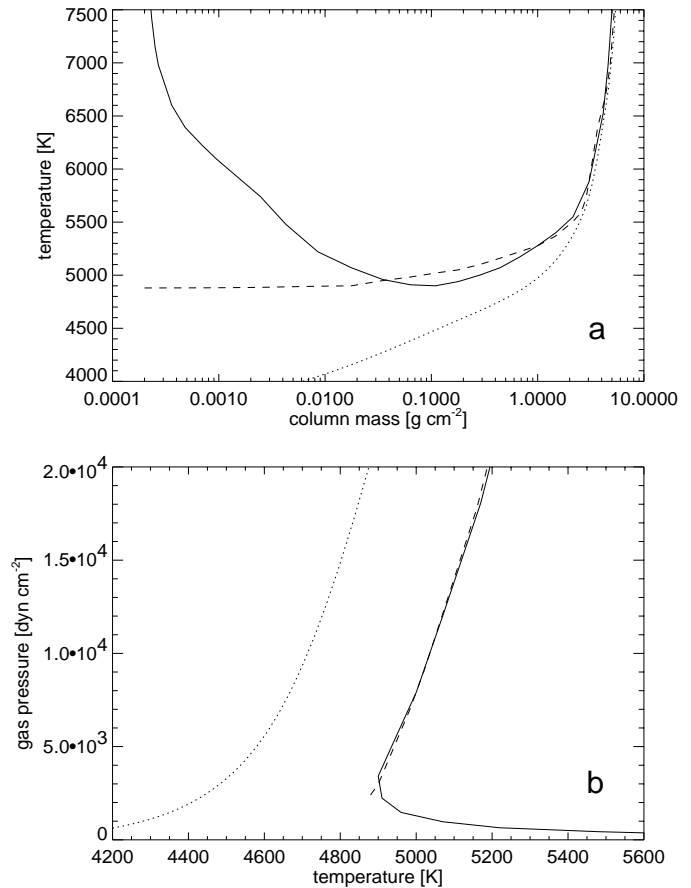


**Fig. 1a and b.** The original and the modified facular models in comparison: **a** the temperature as a function of column mass; **b** the gas pressure as a function of temperature. The solid lines in both plots show model P as given in Fontenla et al. (1993) and the dashed lines show our current facular model. For comparison, Kurucz's solar model is also plotted using dotted lines.

Our calculated flux-to-intensity ratios are consistently lower (by less than 1%, however) than the measurements of Neckel & Labs (1994). A comparison between measured and modelled CLV of a number of selected filters (plotted in Fig. 2b), indicates that this is mainly due to our lower intensities at intermediate limb angles ( $\mu \approx 0.3$  to 0.6). Apparently, small departures from radiative equilibrium are present in the solar atmosphere, which is not surprising in view of the presence of solar convection.

The calculated disk-centre intensities also agree reasonably well with the disk centre measurements by Neckel & Labs (1984) and Burlov-Vasiljev et al. (1998a, 1998b). In the blue, our calculations are somewhat closer to the measurements by Neckel & Labs (1984), but they show better agreement with the data by Burlov-Vasiljev et al. (1998a) in the red. The average deviation between the calculated and measured fluxes over the range of 330 to 1050 nm is of the order of 1.5% for both data sets, the deviation between the two observed intensity sets being 0.8%. When only the wavelength range between 450 and 1050 nm is taken into account, the deviation between all three datasets is below 0.7%.

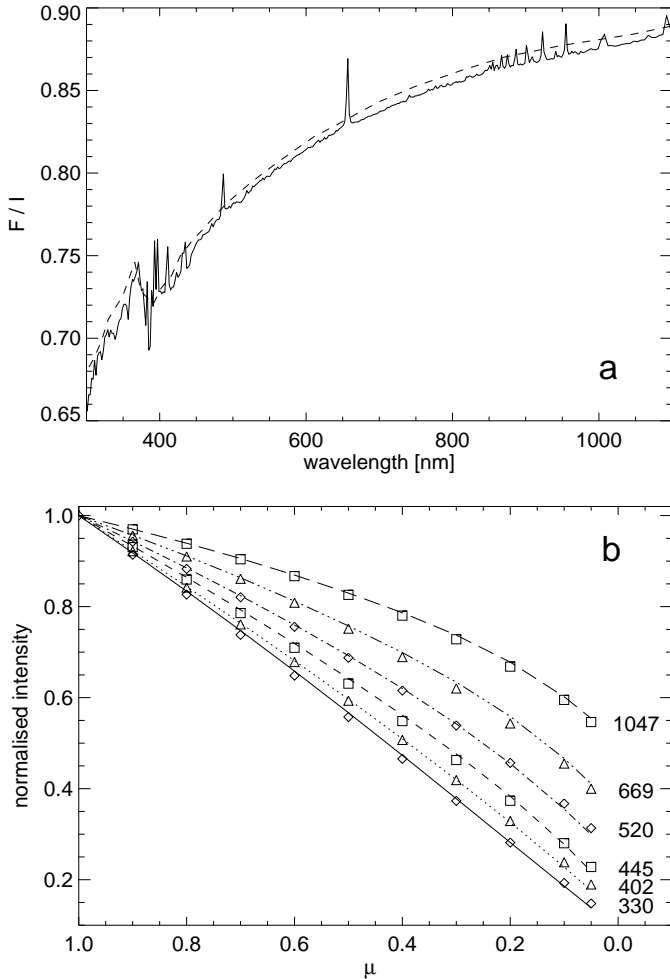


**Fig. 2.** **a** The dashed line shows the disk-integrated flux of the Sun divided by the intensity at disk centre as measured by Neckel & Labs (1994). The solid line shows the same quantity as calculated with ATLAS9 and Kurucz's solar model atmosphere. **b** The CLV of the quiet-sun flux for a number of selected filters. The lines show the fits from Neckel & Labs (1994), the symbols show the intensities obtained with ATLAS9. The numbers next to each line indicate the central wavelength of the narrow-band filters in nm.

## 4. The facular intensities

### 4.1. Centre-to-limb variation

Although the rough behaviour of the facular contrast as a function of limb angle is well established, there is disagreement concerning the details. The contrast is in the following defined as  $(I_f - I_q)/I_q$ , where  $I_f$  is the intensity of the faculae and  $I_q$  the intensity of the quiet Sun. In general, the contrast is low at disk centre, (at IR wavelengths sometimes even negative for sufficiently large magnetic filling factors; Foukal et al. 1990; Wang et al. 1998), and increases out to limb angles of at least  $\cos \theta = 0.3$  (Frazier 1971; Stellmacher & Wiehr 1973; Chapman & Meyer 1986). But there is considerable debate as to whether the contrast continues to increase towards the limb as suggested by the measurements of Lawrence & Chapman (1988) and Taylor et al. (1998), or whether the contrast peaks

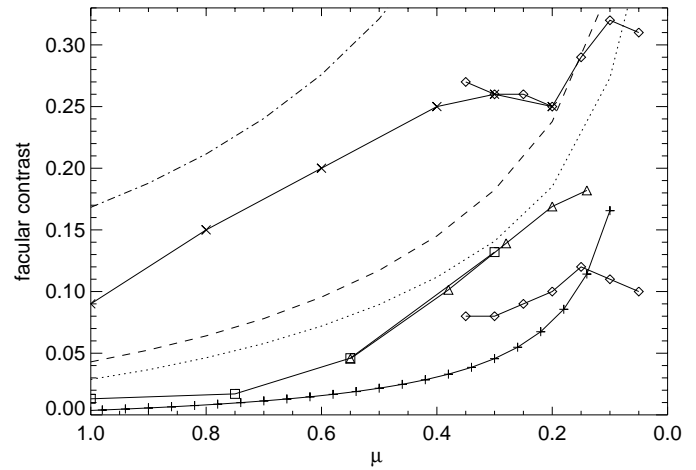


**Fig. 3.** Selected facular contrast measurements,  $(I_f - I_q)/I_q$ , as well as contrasts calculated using our model, plotted vs.  $\mu = \cos \theta$ , where  $\theta$  is the angle between surface normal and the line of sight.  $I_f$  and  $I_q$  are the facular and quiet-sun intensity respectively. The solid lines linking the different symbols show the measurements of facular contrast. The squares, crosses, diamonds and triangles indicate data by Frazier (1971), Auffret & Muller (1991), Wang & Zirin (1987) and Taylor et al. (1998) respectively. The curve linking the plus signs is the parameterisation adopted by Lawrence (1988) for his measurements taken with a filter centred at 524.5 nm. For the Wang & Zirin measurements, the set with the higher contrast values was taken with a filter centred at 386 nm, the lower set with a filter centred at 525 nm, although the passband was not specified. The measurements by Taylor et al. (1998) are in arbitrary units. We have normalised them so that they agree with the measurements by Frazier at  $\mu = 0.55$ . The dotted, dashed and dot-dashed curves are the calculated contrasts in different filters. The dotted line is for 572–578 nm, representative of the filter used by Auffret & Muller; the dashed line is for 470–550 nm. Above 500 nm, the contrast hardly depends on the filter width. The dashed line should therefore be representative for the measurements by Frazier (1971), Lawrence (1988) and the lower set of Wang & Zirin (1987) that were all taken with a green filter. The dot-dashed line is for a filter centred at 386 nm. In this wavelength region, the filter width becomes very important – changing the passband from 50 nm to 10 nm predicts contrasts that are almost twice as high.

at around  $\mu = 0.25$  to  $0.3$  and then decreases again towards the limb (Libbrecht & Kuhn 1984; Auffret & Muller 1991).

Fig. 3 shows a selection of contrast observations, as well as our calculations. This figure illustrates some of the problems that arise when trying to use observed contrast values in order to constrain facular models. The contrast not only depends on the wavelength (as can be seen by comparing the two data sets corresponding to different wavelengths of Wang & Zirin 1987), but also on the magnetic filling factor or average field strength, and very significantly on spatial resolution (compare the curve of Auffret & Muller 1991 with that of Frazier 1971). Obviously, a good fit to all the data is not possible, or even physically desirable with a single model.

In order to correctly reproduce most facular contrast measurements, one would have to construct a complex, comprehensive model that includes the fine structure in the faculae,

i.e. magnetic flux tubes located at the boundaries of (abnormal) granules. For this, one has to know the geometry (size, expansion with height, Wilson depression, see e.g. Spruit 1976), and the correct temperature structure inside the magnetic features (e.g. Bellot-Rubio et al. 1997, Briand & Solanki 1998, Frutiger & Solanki 1998) as well as in their surroundings. The variation of these quantities, e.g. size (Spruit & Zwaan 1981, Keller 1992, Grossmann-Doerth et al. 1994) and temperature (Solanki & Stenflo 1984, Solanki & Stenflo 1985, Solanki & Brigljević 1992), with the amount of flux must be included. Finally, the emerging spectrum from the model for the magnetic filling factor (usually unknown because unmeasured) that is appropriate to the observations must be calculated including the spectral lines and then filtered with the same filter profile as underlies the observations. The magnetic filling factor is the fraction of a given part of the solar surface covered by magnetic field.

This is obviously a daunting task. And even after all this effort, it is likely that success will only be partial, due to the incompatibility between the various observations, and the often unknown magnetic filling factor, spatial resolution and filter function appropriate to the observations.

The facular model we use is one-dimensional and hence neglects all the fine-scale structure. It corresponds to a given (but uncalibrated) magnetic filling factor. Our main aim in this paper is to carry out the last step of the procedure outlined above, namely to calculate the spectral contrast as well as its centre-to-limb variation and compare it with measurements of this quantity (see Sect. 4.2)

The general centre-to-limb variation of the calculated contrast agrees reasonably well with the measurements by Frazier (1971) and Stellmacher & Wiehr (1973) (not shown, but similar to that of Frazier), though our contrast values tend to be higher at disk centre. The absolute value of the contrast probably just reflects the different magnetic filling factors underlying the observations and the model. Frazier (1971) has shown that the facular contrast increases with increasing spatially averaged magnetic field strength, which is equivalent to the magnetic filling factor. His measurements for the faculae with the strongest field strengths are in relatively good agreement with the calculations, albeit still lower. The more recent, high-spatial-resolution measurements by Auffret & Muller (1991) (crosses) indicate much larger contrasts, though the limb-dependence of their contrast values are not in very good agreement with our model. Note, however, that their contrast measurements are of the network bright points and not of spatially averaged faculae, as described by our model. Chapman & Meyer (1986) have parameterized their measurements in terms of  $\Delta I/I = b(\mu^{-1} - a)$  and found  $b$  to be about 0.1 when  $a$  was taken to be unity. This yields a much steeper gradient than any other measurements presented here or indeed our calculations. Using the same parameterisation, Lawrence (1988) Lawrence 1988 finds coefficients of  $a = 0.8$  and  $b = 0.018$  at 524.5 nm. The resulting curve (indicated by the plus-signs in Fig. 3) is in good agreement with our calculations, in particular if we take into account that his coefficients are for “average” faculae, as they were determined by linear

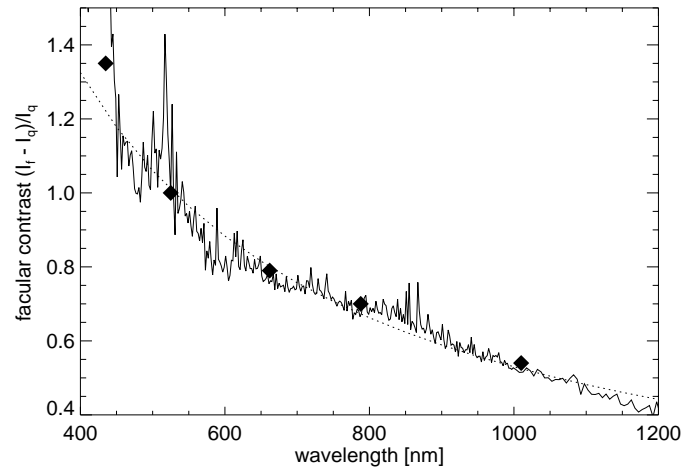


**Fig. 4.** The spectral variation of the facular contrast. The diamonds are the data from Chapman & McGuire (1977). They were obtained from measurements between 16 and 53'' ( $\mu = 0.18$  to 0.33). The dotted line shows the inverse wavelength fit suggested by Chapman & McGuire.

regression to individual measurements that show large scatter. The individual contrast values at  $\mu = 0.2$ , e.g., lie between 2 and 12%. His average curve hence corresponds to a relatively low filling factor.

The steep increase of the contrast near the limb predicted by our model is at least partly the result of the plane-parallel approximation we make. Although this may be an artefact, we do not expect it to seriously influence irradiance reconstructions, since the relative effect of these parts of the solar disc very close to the limb is small, due to their small contribution to the disk area and the limb darkening.

#### 4.2. Colour dependence at a given limb angle

The colour dependence of the facular contrast has been measured by a number of authors, e.g. by Chapman & McQuire (1977) and Lawrence (1988). Chapman & McQuire (1977) measured the facular contrast in five filters between a limb distance of 16'' and 53'', i.e.  $\mu = 0.18$  and 0.33. After normalising the contrasts by setting the contrast value at 530 nm to unity, they found that their data followed an inverse wavelength dependence. We find excellent agreement between our calculations and their measurements. This is shown in Fig. 4 where their normalised contrast measurements (diamonds), the inverse wavelength law (dotted line) and the contrasts calculated from our facular model (solid line) are plotted. Note that the colour dependence of the contrast does not simply scale with changing limb angle. We found that the curves become slightly steeper towards the blue, and show less variation over small wavelength ranges towards the limb. These small-scale spectral variations are due to spectral lines, which show a heightened contrast relative to the continuum most strongly at large  $\mu$ . The effect is relatively small, however, as can be seen from Fig. 5.

Lawrence (1988) measured the contrasts of a large number of faculae, most of them between limb angles of  $\mu = 0.15$  and  $\mu = 0.8$ . As pointed out earlier, the contrast values show

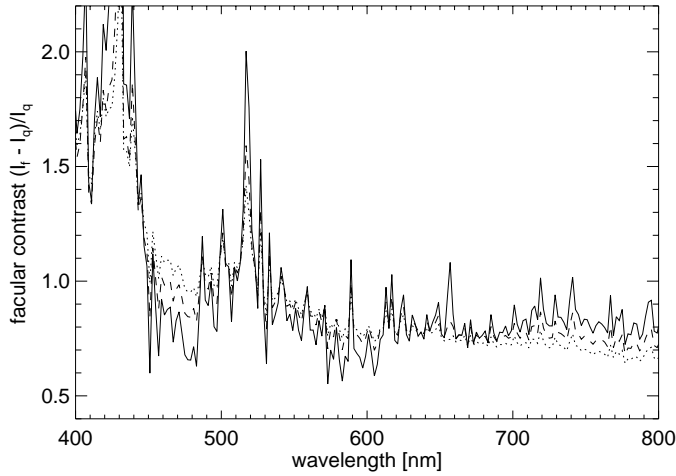


**Fig. 5.** The spectral variation of the facular contrast for different limb angles. The solid line is for the disk centre, the dashed and the dotted lines are for limb angles of  $\mu = 0.6$  and  $0.3$  respectively. The contrasts have all been normalised to be unity at  $530$  nm. At  $530$  nm, the contrast at the disk centre is about  $1.3$  and  $2.5$  times smaller than at  $\mu = 0.6$  and  $0.3$  respectively.

a large scatter (probably for some of the reasons mentioned in Sect. 4.1). When the contrasts in the different wavelength bands are plotted against each other, the scatter is reduced noticeably, and the ratios between the colour contrasts can be calculated. This confirms our suspicion that a large part of the scatter in the contrast measurements is due to different magnetic filling factors.

These ratios (for three different filters) are shown as the solid lines in Figs 6a to c, along with an indication of the error on the slope (dotted lines). Our calculations of the ratios for the different limb angles are in good agreement with the measurements; they are plotted as the diamonds on Figs 6a to c. We stress that the model (i.e. the temperature stratification) was not in any way optimised by us to fit either of these data sets<sup>1</sup>. Note that the inclusion of line blanketing (via the ODFs) in our modelling is of crucial importance for the reproduction of the spectral contrast.

## 5. Flux variations

After investigating the limb behaviour of the faculae, we tested how well the flux spectrum, determined by adding together appropriately weighted intensity spectra, would agree with our previous simpler approach when fitting the spectral variation of the disk-integrated flux (Papers I and II). To this end we compared a three-component model with the irradiance variations as compiled by Lean (Lean 1997 and priv. comm) and with the measurements from VIRGO (see also Fligge et al. 1998). Finally, we also checked for agreement with the results of Mitchell

<sup>1</sup> The spectral dependence of the facular contrast measured by Wang & Zirin (1987) differs very strongly from that measured by Chapman & McGuire (1977) and by Lawrence (1988). Hence it is also not well reproduced by our model. One possible source of the discrepancy is the unknown filter width of the Wang & Zirin (1987) data, which can significantly affect the contrast value of the lower wavelengths.

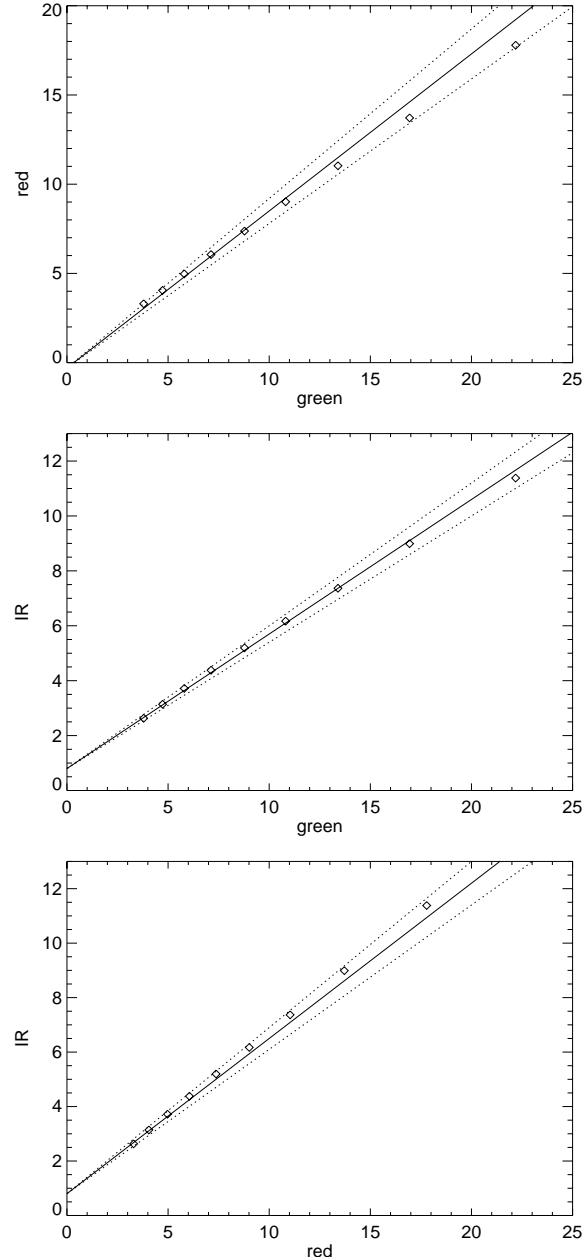


**Fig. 6.** Facular contrasts in percent for three different colour filters (green, red and IR, see Lawrence 1988) plotted against each other. The solid lines are the ratios derived from the contrast measurements of Lawrence (1988), along with his error estimates (dotted lines). The diamonds are our calculated contrasts. The diamonds with the highest contrast values are for a limb angle of  $\mu = 0.2$ . The y-axis offsets of the ratios are arbitrary, as they could not be derived from the measurements by Lawrence (1988).

& Livingston (1991), who estimated the contribution of the spectral lines to the irradiance variations.

### 5.1. Ultraviolet spectral irradiance variations

The irradiance variation between solar-activity maximum and minimum as a function of wavelength are shown in Fig. 7. The

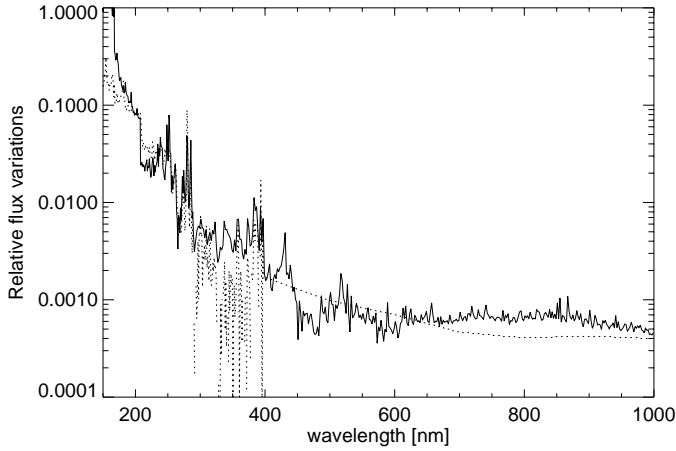


**Fig. 7.** Relative flux (or equivalently irradiance) variations over the solar cycle vs. wavelength. The dotted curve represents observations for wavelengths shorter than 400 nm. The solid line shows the relative irradiance variations resulting from a 3-component model with a facular filling factor of 2.3% and a spot filling factor of 0.23%. The total irradiance variation predicted by the model is 0.1%.

dotted line shows the UV data as compiled by Lean (1997) for wavelengths smaller than 400 nm, and beyond 400 nm her estimate of the flux variations. The solid line is our model fit assuming a global facular filling factor of 2.3% and a spot filling factor of 0.23%. These filling factors were obtained by minimising  $\chi^2$  between the observations and the model between 200 and 400 nm while requiring the total irradiance variation to be 0.1%, according to the ACRIM (Willson & Hudson 1991) and ERB (Kyle et al. 1994) measurements. As no error estimates were available, and so as to avoid overemphasizing the spectral ranges with the largest variations, we arbitrarily set the errors to a fixed fraction of the measured variations.

The fit between 300 and 400 nm is not quite as good as in Paper I where we used a much simpler model. One of the reasons for this is that the flux is now formed over a larger height range, so that changes of individual temperature-depth points in the model atmosphere no longer affect relatively narrow and well-defined wavelength regions. In addition, the observations are also rather unreliable in this particular wavelength range (G. Rottman, priv. comm.). Furthermore, we cannot expect to obtain accurate results in the UV with a strict LTE approach. This problem becomes particularly acute for the shortest wavelengths, where the radiation comes from the highest layers. For these wavelengths the NLTE approach of Fontenla et al. (1999) is certainly to be preferred.

The ratio of facular to sunspot filling factor is around 10, which is only slightly less than what was measured by Chapman et al. (1997) around activity maximum.

## 5.2. VIRGO data

Following Paper II, we compare the output of the new model calculations with time series of total and spectral irradiance obtained with the VIRGO (Variability of Irradiance and Gravity

**Table 1.** Ratio between the RMS variation of the total ( $\sigma_t$ ), red ( $\sigma_r$ ), green ( $\sigma_g$ ) and blue ( $\sigma_b$ ) colour channels for the observed (by VIRGO) and modelled time-series, respectively.

	$\sigma_r/\sigma_t$	$\sigma_g/\sigma_t$	$\sigma_b/\sigma_t$	$\sigma_g/\sigma_b$
VIRGO	0.76	1.31	1.81	0.72
Model	0.85	1.31	1.81	0.72

Oscillations, Fröhlich et al. 1997) instrument onboard SOHO. The time variations of facular and sunspot filling factors are assumed to follow the Mg II k index and sunspot areas, respectively. The details are given in Paper II. We follow that paper exactly, except for the way that the quiet-sun, facular and sunspot flux spectra are constructed.

The resulting model time series of the total solar irradiance and of the irradiance at the three VIRGO wavelength bands look very similar to the time series plotted in Fig. 5 of Paper II and are not plotted again here. A quantitative comparison of the time series shows that due to the increased variations around 400 nm the fit for VIRGO's blue channel is improved. The total, green and blue channels can now be fitted consistently within less than 1% deviation from the RMS variations of the measured time series. Unfortunately, however, the same fit leads to variations of the red channel which are clearly too large (by more than 10%) compared to the measurements.

Therefore, if all four channels are weighted equally, the overall agreement between the reconstructed and the observed time series is of the order of 4–5% only and the reconstructed solar total and spectral irradiance variations are of the same quality as the ones presented in Paper II. The results are summarized in Table 1 which shows the ratios between the RMS variation of the different color channels for the observed and modelled time-series, respectively.

We have also reconstructed the total irradiance over the whole time that solar irradiance has been measured and compared it with the composite put together by Fröhlich & Lean (1998). Once again, the results are similar to those presented in Paper II.

## 5.3. Line blanketing

The course of the solar cycle can also be tracked by changes in the line blanketing. The line-blanketing variations during solar cycle 21 have been measured by Mitchell & Livingston (1991) who found that in disk-integrated spectra the spectral lines in the 500 to 560 nm range are on average 1.4% shallower and have 0.8% smaller equivalent widths at solar maximum than at solar minimum. As expected, the blanketing effect was stronger at the blue end of their spectra than at the red end.

The total irradiance variations can be seen as a combined effect of the flux variations from the continuum and those of the lines. In the following, we define the line blanketing as the ratio of the average absorbed irradiance to the average continuum irradiance in the unblanketed spectrum. In the wavelength range between 500 and 560 nm, Mitchell & Livingston (1991) measured the line blanketing to be 0.076 and the change in the

**Table 2.** The relative flux changes (in percent) of the continuum and emergent spectrum (including lines) due to faculae and spots in different wavelength ranges. The columns and symbols are explained in the text.

1	2	3	4	5	6	7	8	9	10
$\lambda$	$\Delta F_f/F$	$\Delta F_s/F$	$\Delta F_f/F$	$\Delta F_s/F$	$\Delta F/F$	$\Delta F/F$	$\Delta F/F$	line blanketing	spectrum
nm	continuum		spectrum		continuum	spectrum	line	contrib. to total	$\Delta I$
	(%)	(%)	(%)	(%)	(%)	(%)	(%)	(%)	(%)
300–400	0.79	–45.97	26.68	–67.45	–0.089	0.467	–0.553	37.3 (44.2)	31.5 (39.9)
400–500	3.14	–44.83	10.54	–51.54	–0.030	0.127	–0.157	21.4 (21.1)	17.3 (15.4)
500–560	4.71	–41.59	8.51	–45.99	0.014	0.094	–0.078	6.4 (5.4)	7.7 (2.9)
164–160000	3.58	–35.36	7.82	–36.48	0.002	0.099	–0.097	97.9	100.0

line blanketing to be  $-0.8 \pm 0.12\%$ . They then calculate that the irradiance change due to the change in line blanketing is  $-0.066 \pm 0.01\%$  in this wavelength range (see their Eq. 17). We use our calculations to proceed the opposite way and calculate the contribution of the line blanketing from the difference between the continuum variations and the variations of the emergent spectra that include the absorption lines via the ODFs. Our aim is twofold. On the one hand, we use the Mitchell & Livingston (1991) data to test our model. On the other hand, since our model covers a far larger wavelength range than their measurements, we can predict the contribution of line blanketing to the total irradiance variations more easily. In both cases the result is only approximate since we use LTE and ODFs to represent the spectral lines.

Table 2 lists the flux changes  $\Delta F_{f,s}/F = (F_{f,s} - F_q)/F_q$ , where the subscripts  $f$ ,  $s$  and  $q$  indicate the facular, spot flux and quiet-sun flux, respectively. The four rows show results for the wavelength ranges of 300 to 400 nm, 400 to 500 nm, 500 to 560 nm, i.e. the one investigated by Mitchell & Livingston (1991), and for the “total” spectral range (164–160 000 nm). The first column gives the wavelength range; Columns 2 and 3 list the flux changes produced by the facular and spot models for the continuum; Columns 4 and 5 the facular and spot changes for the emergent spectrum, and Columns 6 to 8 show the relative flux change produced by the combination of spots and faculae (for filling factors of 0.23 and 2.3% respectively) in the continuum (6), the emergent spectrum (7) and in the line blanketing (8).

Columns 9 and 10 show our calculations of how much the line blanketing and spectral variations in each wavelength range contribute to the total irradiance variations. Column 9 details the contribution of the line blanketing changes alone; Column 10 shows the contribution of the changes in the emergent spectrum (i.e. line plus continuum). The values in parentheses are the estimates by Mitchell & Livingston (1991) based on an assumed facular contrast of 0.02 at disk centre. Whereas Columns 2 to 5 are independent of the facular and spot filling factors, Columns 6 to 10 have been calculated for the filling factors derived from the fits in Sect. 5.1, i.e. for a facular filling factor of 0.023 and a spot filling factor of 0.0023. For the range between 500 to 560 nm, our line-blanketing contribution of  $-0.078\%$  (see Column 8 in Table 2) agrees to better than 20% with the value of  $-0.066\%$  measured by Mitchell & Livingston (1991).

Mitchell & Livingston (1991) also estimate the percentage contribution of the line blanketing and of the continuum vari-

ations to the total irradiance changes as measured by ACRIM. Their estimates for the continuum contribution are very sensitive to the assumed contrast function for the faculae, so that they list two sets of results, one for faculae that show no contrast at disk centre, and one where the contrast at disk centre is 0.02. The latter is the one our models (that have a contrast of about 0.04 at disk centre) should be compared to. (The continuum contributions are mainly due to spots and are hence negative. For higher facular contrasts the overall continuum contributions will consequently be smaller.)

The predictions of our models are listed in the last two columns of Table 2, the values in parentheses are the results of Mitchell & Livingston (1991), who adopted a facular filling factor of 0.033. Considering the approximative nature of the extrapolations by Mitchell & Livingston (1991) to shorter wavelength ranges and the uncertainties that are introduced into our calculations by considering ODFs only, the agreement between the two data sets is reasonably good.

Of particular interest is the line-blanketing contribution to the total irradiance variations. If our models are to be believed, then continuum variations are negligible and contribute only to a small amount to the total irradiance variations. We have to point out, however, that the exact contributions of the continuum are very model-dependent, particularly so at UV wavelengths, where they cannot be checked against observations due to the flux redistribution into the UV. The contributions of the line blanketing depend to a certain extent on the contrast and on the temperature stratification. If we choose a slightly different stratification (which still reproduces the observations almost as well), the contribution of the line blanketing to total irradiance variations is decreased to 90%. We cannot as yet rule out that line blanketing variations may contribute as little as 70 to 80% to total irradiance variations, but values much below these appear unlikely.

The reason for the dominance of the line blanketing is that most of the continuum-flux increase due to faculae is cancelled out by a corresponding decrease due to sunspots. If the sunspot and facular filling factors were of similar magnitude, the main variations would be due to changes in the continuum and the line changes would approximately cancel each other out. As the facular filling factor is about an order of magnitude larger, the continuum variations due to faculae and sunspots almost cancel out (see Columns 2 and 3) and the line-blanketing change

introduced by the faculae becomes the dominant contribution to the total irradiance variation.

## 6. Discussion and conclusions

We have modelled the facular, quiet-sun and spot intensities of the Sun using Kurucz' ATLAS9 spectral synthesis program. The model for the facular atmosphere is a modified version of model P of Fontenla et al. (1993). The model atmospheres for the quiet Sun and the spots were standard Kurucz radiative equilibrium model atmospheres. Using this much more realistic approach, we confirm our previous conjecture (Papers I and II) that a 3-component model can adequately fit the spectral irradiance variations in the UV, in the visible as measured by VIRGO and the total irradiance variations as measured by ACRIM.

We also check how well our facular model performs when compared to measurements resolving the solar disc. Our calculated facular contrasts as a function of limb angle fit into the general picture of the measurements, though we tend to find larger contrasts than indicated by most of the measurements. However, the scatter between measurements by different groups is large and the absolute contrast values are highly dependent on the resolution of the measurements, the magnetic filling factor of the observed region, and on the technique employed to derive the contrasts (see Solanki 1994 for a more detailed discussion). We find a steeper increase of the contrast very close to the limb, compared to a number of measurements, mainly due to the assumption of a plane-parallel atmosphere. The exact contrast behaviour very close to the limb, however, is not going to be crucially important when modelling the disk-integrated irradiance variations as the flux contribution beyond  $\mu = 0.2$  is very small.

One of the main new features of the modelling described in this paper is that we can reconstruct the spectral dependence of the facular contrast. The calculated colour dependence of the contrast at various limb angles matches the available data very well, suggesting that our approach is not only adequate in a global sense (i.e. in reproducing spectral irradiance variations), but also locally. The inclusion of the influence of spectral lines plays an important role in reproducing these data.

The other significant new result of this paper is that we estimate the influence of line blanketing on irradiance variations in different wavelength ranges. Our model reproduces the observations of Mitchell & Livingston (1991), who estimate the change in line blanketing over the solar cycle from observed spectra, relatively well. Finally, we find that the line blanketing is the major contributor to the total irradiance variations on solar-cycle time scales. The reason is that the sunspot and facular contributions to continuum variations cancel each other out to a large degree, whereas the line-blanketing is changed by sunspots by a much smaller amount than by faculae.

*Acknowledgements.* Dr. J. Lean kindly provided us with her compilation of the observed UV spectral irradiance variations, which we gratefully acknowledge. We are also grateful to CCP7 for the provision of a UNIX version of ATLAS. YCU would like to acknowledge support through the Fond zur Förderung der wissenschaftlichen

Forschung under grant S7302-AST. The work of MF was supported by the Schweizerische Nationalfonds under grant No. 21-40428-94.

## References

- Auffret H., Muller R., 1991, A&A 246, 264  
 Bellot Rubio L.R., Ruiz Cobo B., Collados M., 1997, ApJ 478, L45  
 Briand C., Solanki S.K., 1998, A&A 330, 1160  
 Burlov-Vasiljev K.A., Matvejev Y.B., Vasiljeva I.E., 1998a, In: Hall J.C. (ed.) Solar Analogs: Characteristics and Optimum Candidates. Second Annual Lowell Observatory Fall Workshop, p. 115  
 Burlov-Vasiljev K.A., Matvejev Y.B., Vasiljeva I.E., 1998b, Solar Phys. 177, 25  
 Castelli F., Kurucz R.L., 1994, A&A 281, 817  
 Chapman G.A., McGuire T.E., 1977, ApJ 217, 657  
 Chapman G.A., Meyer A.D., 1986, Solar Phys. 103, 21  
 Chapman G.A., Cookson A.M., Dobias J.J., 1997, ApJ 482, 541  
 Fligge M., Solanki S.K., Unruh Y.C., Fröhlich C., Wehrli C., 1998, A&A 335, 709 (Paper II)  
 Fontenla J.M., Avrett E.H., Loeser R., 1993, ApJ 406, 319  
 Fontenla J.M., White O.R., Fox P.A., Avrett E.H., Kurucz R.L., 1999, ApJ, in press  
 Foukal P., Little R.J.G., Rabin D., Lynch D., 1990, ApJ 353, 712  
 Foukal P., Harvey K., Hill F., 1991, ApJ 383, L89  
 Frazier E.N., 1971, Solar Phys. 21, 42  
 Fröhlich C., Lean J., 1998, In: Deubner F.L. (ed.) New Eyes to see inside the Sun and Stars. IAU Symp. 185, Kluwer Academic Publ., in press  
 Fröhlich C., Andersen B.N., Appourchaux T., et al., 1997, Solar Phys. 170, 1  
 Frutiger C., Solanki S.K., 1998, A&A 336, L65  
 Grossmann-Doerth U., Knoelker M., Schuessler M., Solanki S.K., 1994, A&A 285, 648  
 Keller C.U., 1992, Nat 359, 307  
 Kuhn J.R., Libbrecht K.G., 1991, ApJ 381, L35  
 Kuhn J.R., Libbrecht K.G., Dicke R.H., 1985, ApJ 290, 758  
 Kuhn J.R., Libbrecht K.G., Dicke R.H., 1988, Sci 242, 908  
 Kurucz R.L., 1992a, Rev. Mex. Astron. Astrofis. 23, 45  
 Kurucz R.L., 1992b, Rev. Mex. Astron. Astrofis. 23, 181  
 Kurucz R.L., 1992c, Rev. Mex. Astron. Astrofis. 23, 187  
 Kyle H.L., Hoyt D.V., Hickey J.R., 1994, Solar Phys. 152, 9  
 Lawrence J.K., 1988, Solar Phys. 116, 17  
 Lawrence J.K., Chapman G.A., 1988, ApJ 335, 996  
 Lean J., 1997, ARA&A 35, 33  
 Libbrecht K.G., Kuhn J.R., 1984, ApJ 277, 889  
 Mitchell W.E.J., Livingston W.C., 1991, ApJ 372, 336  
 Neckel H., Labs D., 1984, Solar Phys. 90, 205  
 Neckel H., Labs D., 1994, Solar Phys. 153, 91  
 Solanki S.K., 1994, In: Pap J., Fröhlich C., Hudson H.S., Solanki S.K. (eds.) IAU Colloquium 143: The Sun as a Variable Star: Solar and Stellar Irradiance Variations. Cambridge University Press, Cambridge, p. 226  
 Solanki S.K., Brigljević V., 1992, A&A 262, L29  
 Solanki S.K., Stenflo J.O., 1984, A&A 140, 185  
 Solanki S.K., Stenflo J.O., 1985, A&A 148, 123  
 Solanki S.K., Unruh Y.C., 1998, A&A 329, 747  
 Spruit H.C., 1976, Solar Phys. 50, 269  
 Spruit H.C., Zwaan C., 1981, Solar Phys. 70, 207  
 Stellmacher G., Wiehr E., 1973, A&A 29, 13  
 Taylor S.F., Varsik J.R., Woodard M.F., Libbrecht K.G., 1998, Solar Phys. 178, 1  
 Wang H., Zirin H., 1987, Solar Phys. 110, 281  
 Wang H., Spirock T., Goode P.R., et al., 1998, ApJ 495, 957  
 Willson R.C., Hudson H.S., 1991, Nat 351, 42